An Elastic Damage Model for the Simulation of Recoverable Polymeric Foams

S. Kolling[1], A. Werner[2], T. Erhart[3], P.A. Du Bois[4]

[1] DaimlerChrysler AG, EP/SPB, HPC X271, D-71059 Sindelfingen, Germany

[2] Northeastern University, Department of Structural Engineering, Boston, MA 02115, USA

[3] Dynamore GmbH, Industriestr. 2, D- 70565 Stuttgart, Germany

[4] Consulting Engineer, Freiligrathstr. 6, 63071 Offenbach, Germany

Abstract:

Simulation of recoverable foams is usually based on hyperelasticity. Since foams are always strain-rate dependent, the viscosity of the material has to be considered additionally in the material model. One disadvantage of a viscous description is the time-consuming parameter identification associated with the determination of the damping constants. An alternative is given by tabulated formulations where stress-strain relations based on uniaxial static and dynamic tensile tests at different strain rates are used directly as input. This approach is implemented in the material law no. 83 (Fu-Chang-Foam) in LS-DYNA, see [1] and [2]. We briefly show the theoretical background and the algorithmic setup of the tabulated Fu-Chang model and demonstrate the applicability of the model to non-uniaxial loading. Major problems occur in the simulation of unloading processes. These difficulties are due to the identification of unloading by the product of strain and strain rate as implemented in material law no. 83 so far. If the strain rate oscillates strongly, a unique identification of loading and unloading is no longer possible. Therefore, an extension of the model with elastic damage is presented that is capable of identifying unloading in a natural way, i.e. by a decrease of the stored hyperelastic energy of the system. With our model, hysteresis effects can be simulated and energy is dissipated. The model is formulated in a user-friendly way by a tabulated description of damage.

Keywords:

Material Modeling, Foams, Hyperelasticity, Strain-rate Dependency, Elastic Damage, parameter identification, Explicit Finite Element Method

1 Introduction

Simulation of soft foams is an important topic in engineering practice and the formulation of the proper deformation mechanism represents an interesting field in academic research, too. The exciting thing (for a numericist) is that foams are not continua but they are open- or closed cell structures. The mechanical properties thus depend upon the geometric structure of the foam (i.e. size and shape of the cells) and the intrinsic properties of the cell wall material. Deformation mechanisms include cell wall bending up to elastic buckling followed by a "plastification" phase. This behavior is reversible in soft polymer foams, hence the notation "recoverable foam". The range of application goes from door and pillar paddings, dummy components (confor foam on EUROSID ribs), seat cushions, bumpers to mattresses.In open cell structures, the property of the contained fluid has an effect on the mechanical response [3]. For the numerical treatment of such foams, see [4] and [5].
In this paper, we describe the material behavior in a phenomenological way by hyperelasticity and size effects are thus neglected. The chosen approach considers the foam as a continuum and the foam's macroscopic behavior is reproduced. This method has been successfully used in many applications [6], [7], [8]. If strain-rate dependency has to be considered, viscous dampers also have to be taken into account in the material model. A disadvantage of such a description is time-consuming parameter identification associated with the damping constants. In the LS-DYNA implementation according to Fu Chang [9], a tabulated formulation is used which allows a fast generation of the input data based on uniaxial static and dynamic tensile tests at different strain rates. In an extension of this material law, we use an elastic damage formulation for the modeling of the unloading behavior, i.e. forming of a hysteresis during cyclic loading, see [10] for the theoretical background. The model is likewise formulated in a user-friendly way by a tabulated description of the damage curve as shown in [11] and [12]. We show the basic equations and algorithmic setup of our model which has been implemented in LS-DYNA 971.

2 Current Implementation According to Fu Chang

2.1 Theoretical Framework

The numerical simulation of foam materials is based on a tabulated approach of hyperelasticity formulated in the principal (true) stress space. In LS_DYNA the case for a material with uncoupled principal engineering stresses (=foam) is covered in MAT_083 or MAT_FU_CHANG_FOAM. For clarity the algorithm will be briefly summarized. We limit this to the case where the stress-strain curve covers both the compressive and the tensile region (TFLAG=1) and the computation of stresses consequently makes no distinction between tension or compression. A slightly simplified formulation with linear stress-strain relationship in tension (TFLAG=0) is also available in the code but not treated here. The algorithm under consideration then proceeds as follows:

1. Compute the square of the left stretch tensor **V** from the deformation gradient **F**:

$$\mathbf{V}^2 = \mathbf{F}\mathbf{F}^T \tag{1}$$

2. Diagonalize the left stretch tensor by computing the eigenvectors arranged in the matrix $\mathbf{\Phi}$ and compute the principal stretch ratios λ_i:

$$\boldsymbol{\lambda}^2 = \mathbf{\Phi}^T\mathbf{V}^2\mathbf{\Phi} = \begin{pmatrix} \lambda_1^2 & 0 & 0 \\ 0 & \lambda_2^2 & 0 \\ 0 & 0 & \lambda_3^2 \end{pmatrix} \Rightarrow \boldsymbol{\lambda} = \begin{pmatrix} \lambda_1 & 0 & 0 \\ 0 & \lambda_2 & 0 \\ 0 & 0 & \lambda_3 \end{pmatrix} \tag{2}$$

3. Compute the strain rates via velocity gradient **L** in the principal directions of the left stretch tensor

$$\dot{\varepsilon} = \frac{1}{2}\left(\mathbf{L} + \mathbf{L}^T\right)$$
$$\dot{\boldsymbol{\lambda}} = \boldsymbol{\Phi}^T \dot{\varepsilon} \boldsymbol{\Phi} = \begin{pmatrix} \dot{\lambda}_1 & 0 & 0 \\ 0 & \dot{\lambda}_2 & 0 \\ 0 & 0 & \dot{\lambda}_3 \end{pmatrix} \tag{3}$$

4. Filter the principal strain rate values. Here we use a simple or running 12point averaging scheme (SRAF=1/0):

$$\lambda_i^{ns} = \sum_{m=n-11}^{n} \frac{\lambda_i^m}{12} \qquad \mathrm{SRAF} = 1$$
$$\lambda_i^{nr} = \frac{\lambda_i^n}{12} + \sum_{m=n-11}^{n-1} \frac{\lambda_i^{mr}}{11} \qquad \mathrm{SRAF} = 0 \tag{4}$$

5. Compute principal engineering strains taking into account that the tabulated stress-strain values are positive in compression and negative in tension

$$\varepsilon_{0i} = 1 - \lambda_i \tag{5}$$

6. Convert strain rates to engineering strain rates if needed (SFLAG=0/1). Set strain rate value to zero in a principal direction if we have unloading:

$$\dot{\varepsilon}_i = \begin{cases} \left|\dot{\lambda}_i\right| & \dot{\lambda}_i \varepsilon_{0i} < 0 \\ 0 & \dot{\lambda}_i \varepsilon_{0i} > 0 \end{cases} \tag{6}$$
$$\dot{\varepsilon}_i = \dot{\varepsilon}_i \left(1 - \varepsilon_{0i} * SFLAG\right)$$

7. Compute principal engineering stresses by a table lookup. The table lookup uses strain and strain rate in each principal direction (RFLAG=1). Then compute principal true stresses that are positive in tension.

$$\sigma_i = -\frac{\sigma_{0i}\left(\varepsilon_{0i}, \dot{\varepsilon}_i\right)}{\lambda_j \lambda_k} \tag{7}$$

8. Compute Cauchy stresses in the global system using the fact that in a hyperelastic material the eigenvectors of the true stress tensor and the left stretch tensor are identical

$$\boldsymbol{\sigma} = \boldsymbol{\Phi} \begin{pmatrix} \sigma_1 & 0 & 0 \\ 0 & \sigma_2 & 0 \\ 0 & 0 & \sigma_3 \end{pmatrix} \boldsymbol{\Phi}^T \tag{8}$$

This summarizes the approach followed in most foam material laws implemented in LS-DYNA and in the popular MAT_083 or MAT_FU_CHANG_FOAM in particular. It has proven to be a valid and useful

tool for the simulation of foam structures under dynamic loading in countless applications. More detail about some of the alternative formulations that were made available can be found in [9].

It has to emphasized, however, that this formulation considers not the real viscosity of the material. The formulation is referred to as “strain-rate-dependent-hyperelasticity” (a nomenclature that is a contradiction in terms) that wangles viscosity in a numerical way.

A further weak point of this material model was recently shown to be the unloading response. The unloading algorithm is incorporated in step 6 above. If the signs of strain and strain rate are opposite the strain rate value is set to zero and the computed stresses are automatically on the lowest curve of the tabulated input data. The approach is in principle numerically stable but the unloading response is rate-independent. In practical applications though, the oscillatory response which is intrinsically linked to elastic behavior causes non-zero strain rate values to be computed during the unloading phase. This will cause too high stress values to be evaluated and rebound velocities of impactors are accordingly overestimated.

In the present study an alternative unloading model is proposed based on a damage formulation. One of the advantages of this formulation is that the unloading response of the material can be rate dependent.

2.2 Validation Tests

In daily engineering practice, experimental data is available for compression and (if any) tensile tests only. This is, of course, sufficient to validate a material card for MAT_83. In this section, we show additionally the accuracy of the Fu Chang model for non-uniaxial loads like shear and torsion. The results are taken from [14].

In a first example, we simulate a compression test as it is shown in Figure 1. The technical stress-strain relation obtained from this can be used directly in MAT_83. As can be seen in Figure 1, the material shows a Poisson coefficient close to zero. This is only the case for low density foams, roughly below 200g/l. High density (>200g/l) structural foams cannot be treated by MAT_83 since they exhibit a non-negligible Poisson effect.

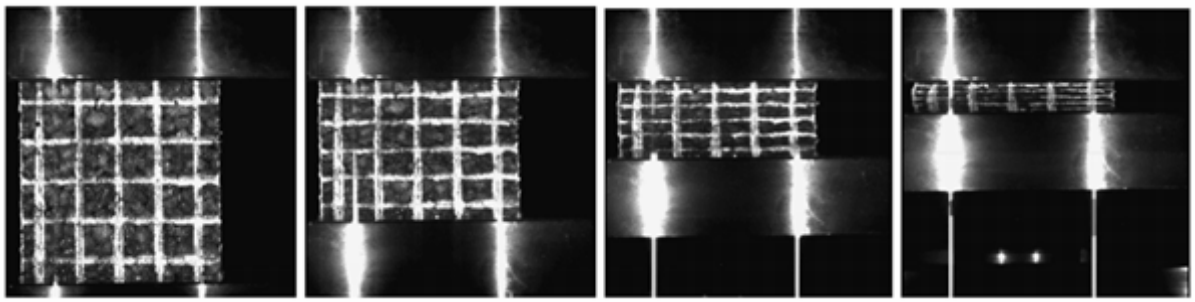

Figure 1: Experimental performance of a compression test

For EPP RG30 (RG denotes the density in g/l) the compression test has been simulated with LS-DYNA. The results of the computation and the corresponding FE-model are given in Figure 2. The loading path can be fitted exactly with MAT_83. Furthermore, the influence of the viscous coefficient DAMP is shown whereas it can be seen that utilizing a DAMP constant of 0.5% leads to a slightly overestimation of the stress level during the loading phase. However, the unloading path cannot be simulated sufficiently. As one can see, in the unloading range the obtained stresses deviate highly from the test results which are caused by the detection algorithm deployed in the material model MAT_83. In Figure 3 the strain rates and node velocities are shown. Looking at the picture clarifies the problem since one can clearly observe the varying positive and negative strain rates which in turn lead simultaneously occurring loading and unloading areas.

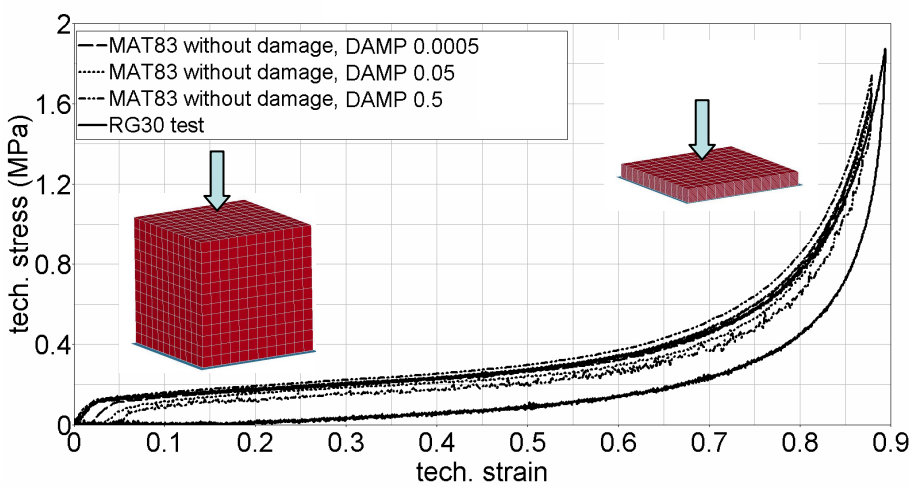

Figure 2: Simulation of a compression test

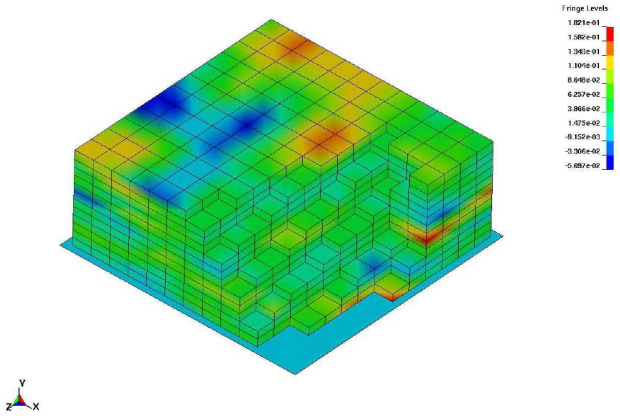

Figure 3: Strain rates compression test unloading phase

In the next example, a tensile test for EPP RG40 is shown. The specimen and the results for two different strain rates are given in Figure 4. The simulations show a good agreement with the experiment given the fact that the results were computed by using input data from different experimental tests. However, the obtained stress strain characteristic is close to the experimental test results. This fact and looking at the loading path results of the compression test simulation where updated experimental test data were used let us reasonable assume that if updated input data would have been utilized the simulation results would have matched the experimental tests very close. Another imported fact should be emphasized namely that EPP shows a non-negligible Poisson effect under tension, see corresponding experimental performance in [18], [19] and [16]. However, tensile stress plays fortunately a secondary role in real structures made from EPP-foam.

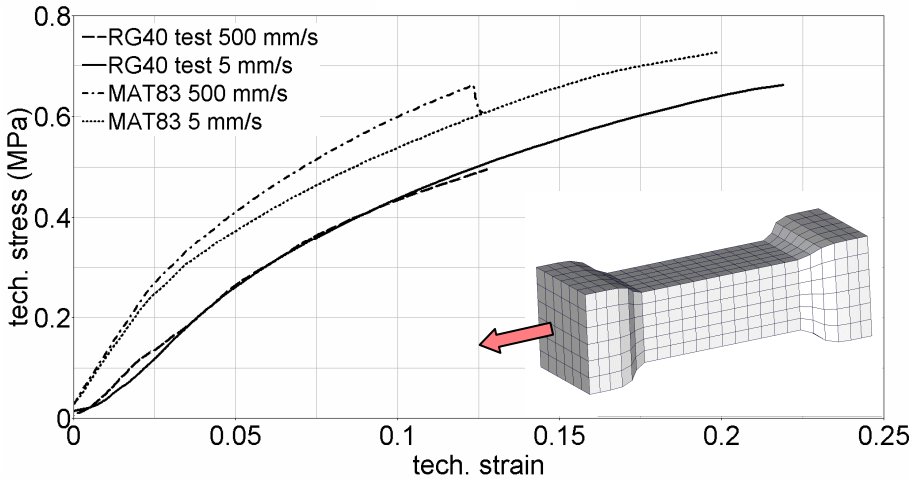

Figure 4: Tensile test

Now we test the input data in non-uniaxial tests. First we consider a shear test as it is shown in Figure 5. The experimental setup consists of two shear test specimens glued with three steel plates. The lower and the upper steel plates are fixed on the right hand side and a prescribed displacement is applied to the middle plate. Thus a simple shear situation is forced.

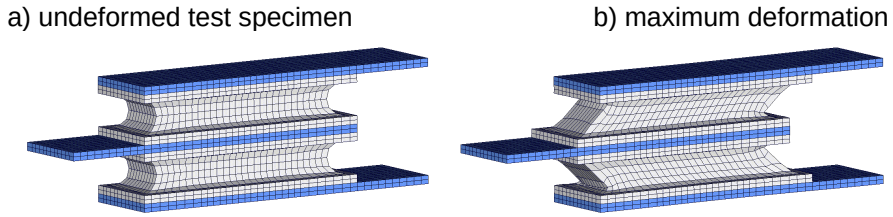

Figure 5: Shear test simulation

The results of the simulation and the experimental data taken from [16] are given in Figure 6. Up to 10mm the simulation is very close to the experiment whereas deviation in initial stiffness can be observed. Furthermore for larger deformation, a softening behavior caused by onset of failure of the tested material can be detected that cannot be simulated with Fu-Chang's foam.

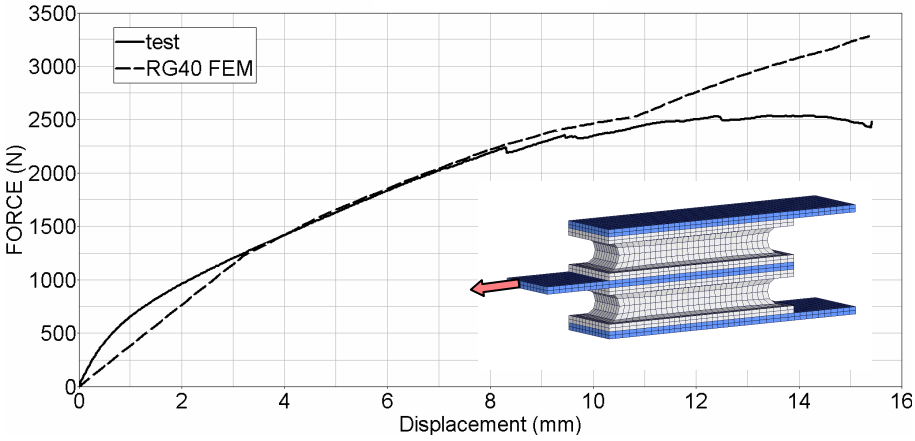

Figure 6: Simple shear test

As a last example, we simulate a torsion test presented by Schlimmer in [19]. Here, a cylindrical foam specimen is glued between two cylinders made from steel, see Figure 7 and Figure 8. With this setup, a wide range of mixed mode loading can be applied. Here a torsion test has been performed where one of the steel cylinders is fixed and the other one performs a rotational motion whereas the longitudinal translational degree of freedom is free. The simulation were conducted incorporating the viscous hourglass formulation available in LS-DYNA. Figure 7 shows the temporal evolution of the torsion test.

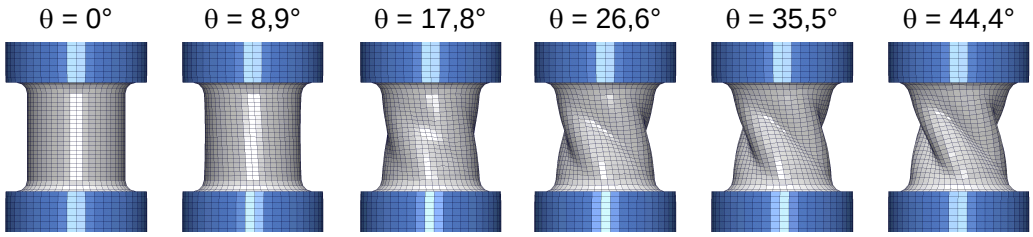

Figure 7: Simulation of a torsion test at different torsion angles

In the experiment, global shear stress and strain as well as the longitudinal strain have been measured. Despite the fact that here a complex state of stress were simulated using a constitutive law based on compression and tensile test data as well as neglecting the Poisson effect results show a very good agreement to the experimental data. The small variation in both obtained result quantities are within a reasonable range and the global behavior of the tested specimen can be modeled sufficiently.

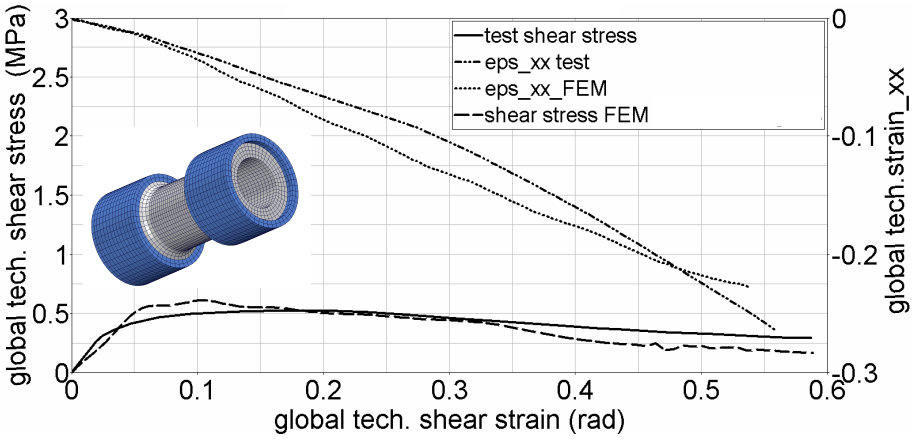

Figure 8: Torsion test

To sum up it can be said that the current implementation of MAT_83 leads to pretty good results in comparison to experiments. It shows the applicability of Fu Chang's foam model for the simulation of structural parts made from soft foam even for more complex stress states. The unloading path due to the hyperelastic model remains the biggest stumbling block. In the next section, we show an extension of the current formulation using elastic damage for unloading simulation.

3 Addition of a Damage Model

3.1 Theoretical Framework

First one must realize that the current formulation of our foam material law is nothing else then a tabulated generalization of a hyperelastic material law based on the Hill functional [13]. Hill gives the energy per unit undeformed volume of the material as

$$W = \sum_{i=1}^{3}\sum_{j=1}^{m}\frac{\mu_j}{\alpha_j}\left(\lambda_i^{\alpha_j} - 1\right) + \frac{1}{n}\sum_{j=1}^{m}\frac{\mu_j}{\alpha_j}\left(J^{-n\alpha_j} - 1\right) \tag{9}$$

The corresponding expression for the true stress is easily obtained by differentiation:

$$\sigma_i = \frac{1}{\lambda_k\lambda_j}\frac{\partial W}{\partial \lambda_i} = \sum_{j=1}^{m}\frac{\mu_j}{J}\left[\lambda_i^{\alpha_j} - J^{-n\alpha_j}\right] \tag{10}$$

The case of a foam material corresponds to setting *n=0* meaning the material has a zero Poisson coefficient, for the engineering stress we then obtain:

$$\sigma_{0i} = \frac{\partial W}{\partial \lambda_i} = \sum_{j=1}^{m}\frac{\mu_j}{\lambda_i}\left[\lambda_i^{\alpha_j} - 1\right] \tag{11}$$

Which is a fully uncoupled expression: any principal engineering stress component in a foam depends solely on the value of the stretch ratio in the corresponding principal direction. The polynomial expression can then be replaced by any continuous tabulated function which can be directly obtained from the test:

$$\sigma_{0i} = \sigma_{0i}\left(\varepsilon_{0i}\right) = \sigma_{0i}\left(1 - \lambda_i\right) \tag{12}$$

Here we have defined the engineering strain to be positive in compression as is usually done for foams. Rate effects are then considered by replacing the single load curve data by a table of load curves corresponding to experiments at different strain rates:

$$\sigma_{0i} = \sigma_{0i}\left(\varepsilon_{0i}, \dot{\varepsilon}_{0i}\right) \tag{13}$$

In the damage model we will need to evaluate the hyperelastic energy as well as the true stress in the material, expressing Hill's functional for *n=0* shows that the energy per unit undeformed volume is also uncoupled in terms of the principal stretch ratios:

$$\begin{aligned}\lim_{n\to 0} W &= \sum_{i=1}^{3}\sum_{j=1}^{m}\frac{\mu_j}{\alpha_j}\left(\lambda_i^{\alpha_j} - 1\right) + \lim_{n\to 0}\frac{1}{n}\sum_{j=1}^{m}\frac{\mu_j}{\alpha_j}\left(J^{-n\alpha_j} - 1\right) \\ &= \sum_{i=1}^{3}\sum_{j=1}^{m}\frac{\mu_j}{\alpha_j}\left(\lambda_i^{\alpha_j} - 1\right) - \sum_{j=1}^{m}\mu_j \ln J \\ &= \sum_{i=1}^{3}\left[\sum_{j=1}^{m}\frac{\mu_j}{\alpha_j}\left(\lambda_i^{\alpha_j} - 1\right) - \sum_{j=1}^{m}\mu_j \ln \lambda_i\right].\end{aligned} \tag{14}$$

Consequently the energy can also be generalized to a sum of 3 tabulated functions of the principal stretch ratios:

$$W = \sum_{i=1}^{3} W_u\left(\lambda_i\right) \tag{15}$$

So in a foam, the energy per unit undeformed volume is uncoupled in the principal directions. It is easily seen that the function W_u corresponds to the energy absorption under uniaxial loading. Indeed uniaxial loading in a foam corresponds to:

$$\lambda_i \neq 1, \;\; \lambda_j = \lambda_k = 1 \tag{16}$$

And thus

$$W_u(\lambda_i) = \sum_{i=1}^{3}\left[\sum_{j=1}^{m}\frac{\mu_j}{\alpha_j}\left(\lambda_i^{\alpha_j} - 1\right) - \sum_{j=1}^{m}\mu_j \ln\lambda_i\right] = \sum_{j=1}^{m}\frac{\mu_j}{\alpha_j}\left(\lambda_i^{\alpha_j} - 1\right) - \sum_{j=1}^{m}\mu_j \ln\lambda_i \tag{17}$$

Consequently, in the generalized case the function W_u is obtained by integration of the engineering stress curve measured in a uniaxial tension/compression test:

$$W_u(\lambda_i) = \int_0^{\lambda_i} \sigma_0(\varepsilon_0)\, d\varepsilon_0 \tag{18}$$

The damage model will now be defined from a quasistatic experiment where loading and unloading path are carefully measured. Tensile and compressive tests should be performed ideally.

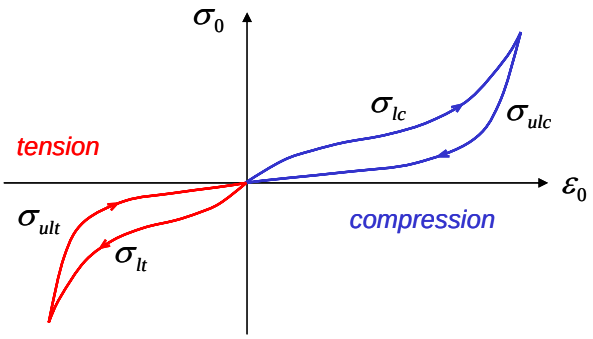

Figure 9: Loading and unloading curves

To each stress strain point on the loading curve corresponds a value of the uniaxial energy obtained by integration. Maximum tensile and compressive deformation correspond to maximum values of the energy in tension and compression: $W_{\max t} \quad and \quad W_{\max c}$

A damage value is then attributed as a function of the current of maximum energy ratios:

$$\varepsilon_0 > 0 \Rightarrow d = d\left(\frac{W}{W_{\max c}}\right) = 1 - \frac{\sigma_{ulc}}{\sigma_{lc}}$$
$$\varepsilon_0 < 0 \Rightarrow d = d\left(-\frac{W}{W_{\max t}}\right) = 1 - \frac{\sigma_{ult}}{\sigma_{lt}} \tag{19}$$

It should be noticed that the energy is set to a negative value in case of tension. This has the advantage that only one damage function will be necessary for the whole range of compression and tension.

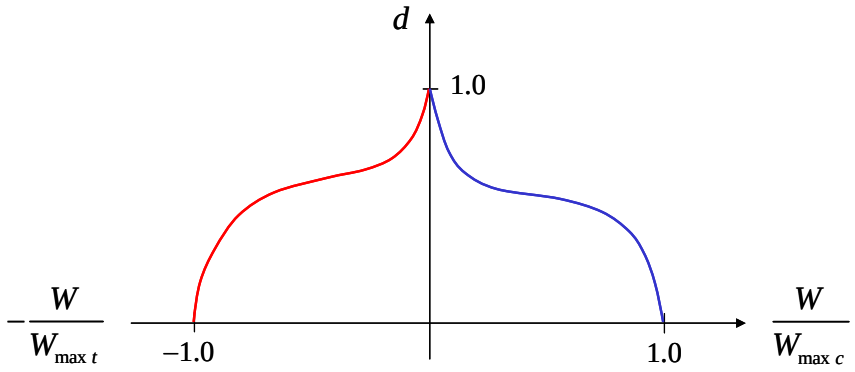

Figure 10: Damage as function of energy ratio (qualitative sketch)

Consequently from the usual tabulated data $\sigma_{0i} = \sigma_{0i}(\varepsilon_{0i}, \dot{\varepsilon}_{0i})$ we will internally derive and store 2 additional load curves: the uniaxial hyperelastic energy $W_u(\varepsilon_{oi})$ and the damage function $d(W/W_{\max})$.

With these additional data available the damage algorithm becomes very efficient and the modifications to the basic algorithm presented earlier are minor. An additional step is created.

5b. Compute quasistatic principal engineering stresses, check if we are in tension or in compression and compute the damage:

$$\begin{aligned}
&\sigma_{oi} = \sigma_{oi}(\varepsilon_{0i}, 0)\\
&W = W_u(\lambda_1) + W_u(\lambda_2) + W_u(\lambda_3)\\
&W_{\max} = \max(W, W_{\max})\\
&J = \lambda_1\lambda_2\lambda_3\\
&J \le 1 \Rightarrow d = d\left(\frac{W}{W_{\max}}\right)\\
&J > 1 \Rightarrow d = d\left(-\frac{W}{W_{\max}}\right)
\end{aligned} \qquad (20)$$

Steps 6 and 7 are then modified as follows:

$$\begin{aligned}
&\varepsilon_{0i} = 1 - \lambda_i\\
&\dot{\varepsilon}_i = \left|\dot{\lambda}_i\right|\\
&\dot{\varepsilon}_i = \dot{\varepsilon}_i(1 - \varepsilon_{0i} * SFLAG)\\
&\sigma_i = -(1-d)\frac{\sigma_{0i}(\varepsilon_{0i}, \dot{\varepsilon}_i)}{\lambda_j\lambda_k}
\end{aligned} \qquad (21)$$

Showing that rate effects are now applied also during unloading and hysteresis is a consequence of the damage mechanism rather then the viscosity. For this model the quasistatic unloading and loading paths should be the first two curves in the table corresponding to very low values of the strain rate. They will then determine the hysteresis and hardly have any influence on the viscosity of the material. For good functioning of the model, it is essential that these two curves form a closed loop, i.e. begin- and endpoint should be identical for both curves.

3.2 Examples

3.2.1 Cyclic loading

At first the effect of the new damage formulation will be shown in a single element test, where compressive uniaxial loading is applied with prescribed motion. Loading and unloading curves are given in tabulated form as closed loop with maximum strain $\varepsilon_{\max} = 0.47$ (see dashed line in Figure 10). As expected, loading can be reproduced exactly with and without the new damage formulation. On the other hand, clear differences are present in case of unloading. Without the damage formulation, strain rate is set to zero if the unloading criterion is met. This results in a sudden jump of the stress path from loading curve to unloading curve. In case of load path 1 with $\varepsilon_{\max} = 0.47$, which exactly matches the prescribed curves, this seems to be no problem. But in case of load path 2 with less deformation ($\varepsilon_{\max} = 0.40$) an unphysical abrupt stress drop can be observed. Load path 3 with higher compression $\varepsilon_{\max} = 0.55$ is even worse, since the jump from loading to unloading curve leads to an increase in stress, which is physical nonsense. With the new damage formulation, we obtain the exact curve as given in the input data again for load path 1. For load paths 2 and 3, the unloading behavior is affine to the prescribed unloading and therefore appears to be reasonable from an engineering point of view.

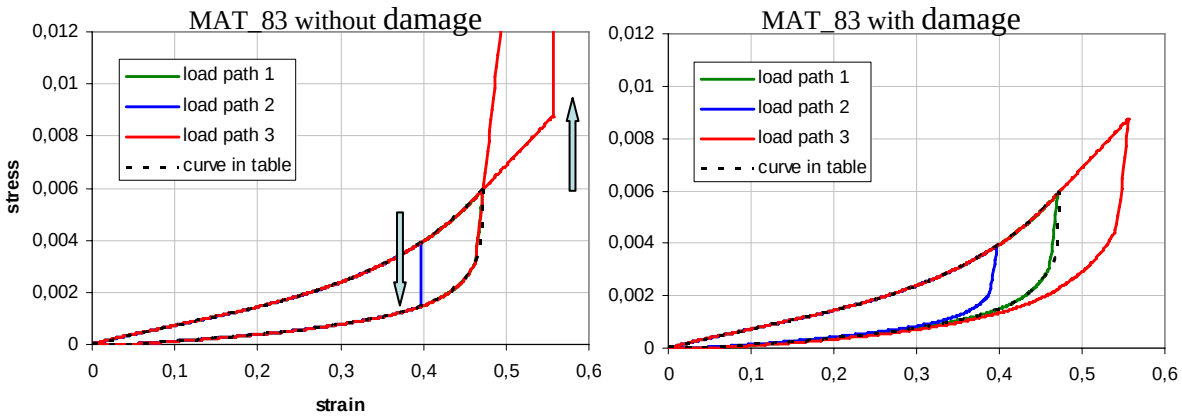

Figure 11: Simulation of cyclic loading with and without damage

3.2.2 Impact test

In this experiment, a rigid sphere (mass 10kg, diameter 135mm) centrally hits a rectangular foam block (RG110, 200x200x40 mm) with an initial velocity of 5.22m/s. After a maximum of penetration is reached, the ball bounces back in the opposite direction.

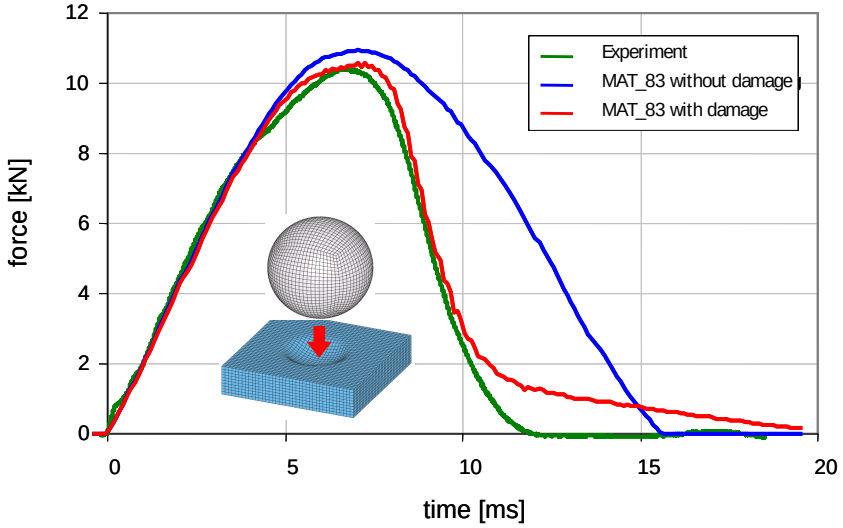

Figure 12: Impact test – experiment vs. simulation with and without damage

Comparing the force over time curves in Figure 11, it gets obvious that the loading phase is well captured with the old and the new formulation. Apparently this is not the case during the rebound phase, which is governed by unloading of the foam material. With the new damage formulation, an enhancement of the simulation result is evident.

4 References

[1] LS-DYNA User Manual and Theoretical Manual, Livermore Software Technology Corporation.

[2] Du Bois, P.A. (2004): Crashworthiness Engineering Course Notes, Livermore Software Technology Corporation.

[3] Mills, N.J.; Gilchrist, A. (2000): The high strain extension of open cell foams. Journal of Engineering Materials and Technology – Transactions of the ASME 122: 67-73.

[4] Ehlers, W. (2002): Foundations of multiphasic and porous materials. In: Ehlers, W., Bluhm, J. (eds.) Porous Media: Theory, Experiments and Numerical Applications, pp. 3–86. Springer-Verlag, Berlin.

[5] Markert, B. (2005): Porous Media Viscoelasticity with Application to Polymeric Foams, Dissertation, Report No. II-12 of the Institute of Applied Mechanics (CE), Universität Stuttgart, Germany.

[6] Du Bois, P.A.; Kolling, S.; Koesters, M.; Frank, T. (2006): Material behaviour of polymers under impact loading. International Journal of Impact Engineering 32: 725-740.

[7] M. Schrodt, G. Benderoth, A. Kuehhorn, G. Silber (2005): Hyperelastic description of polymer soft foams at finite deformations. Technische Mechanik 25 (3-4): 162–173.

[8] Feng, W.W. (2003): On constitutive equations for elastomers and foams. 4th European LS-DYNA Users Conference, pp. D-II-15/28.

[9] Chang, Fu S.; Song, Y; Lu, D.X.; DeSilva, C.N. (1998): Unified constitutive equations for foam materials. Journal of Engineering Materials and Technology – Transactions of the ASME 120 (3): 212-217.

[10] Miehe, C. (1995): Discontinuous and Continuous Damage Evolution in Ogden-Type Large Strain Elastic Materials, European Journal of Mechanics, A/Solids 14: 697–720.

[11] Kolling, S.; Benson, D.J.; Du Bois, P.A. (2005): A simplified rubber model with damage. 4th LS-DYNA Forum, Bamberg, 2005, Conference Proceedings, ISBN 3-9809901-1-7, pp. B-II-01/10.

[12] Kolling, S.; Du Bois, P.A.; Benson, D.J.; Feng, W.W. (2007): A tabulated formulation of hyperelasticity with rate effects and damage. Computational Mechanics, in press, DOI: 10.1007/s00466-006-0150-x.

[13] Hill, R. (1978): Aspects of invariance in solid mechanics, Adv. Appl. Mech. 18: 1-75.

[14] A. Werner (2006): Zur Simulation reversibler EPP-Schäume unter mehrachsiger und stoßartiger Beanspruchung. Diplomarbeit DaimlerChrysler AG, Sindelfingen & BTU Cottbus.

[15] Mills, N.J.; Zhu, H. (1999): The high strain compression of closed-cell polymer foams. Journal of the Mechanics and Physics of Solids, 47:669-695.

[16] Fremgen, C.M.; Huber, U.; Maier, M. (2005): Experimental investigation of polypropylen foams as base for numerical simulation. Cellular Metals and Polymers, Eds.: R. F. Singer et al., Trans Tech Publications, Zürich, Schweiz.

[17] Mills, N.J.; Gilchrist, A. (1999): Shear and Compressive Impact of Polypropylene Bead Foam. Cellular Polymers, 18(3): 157-174.

[18] Huber, U.; Maier, M. (2005): Experimentelle Untersuchung von Polypropylen-Schaum als Basis für die numerische Simulation. Workshop „Simulation von Schaumstoffen mit stark nichtlinearem Verhalten“, Hohenwart, Germany.

[19] Münch, M.; Rohde, S.; Schlimmer, M. (2005): Mehrachsige Beanspruchung von thermoplastischen Konstruktionsschaumstoffen. Workshop „Simulation von Schaumstoffen mit stark nichtlinearem Verhalten“, Hohenwart, Germany.

